ON THE BIAS OF PSEUDOLINEAR ESTIMATORS FOR TIME-OF-ARRIVAL BASED LOCALIZATION

Ngoc Hung Nguyen[⋆] *and Kutluyıl Doğançay*[†⋆]

[⋆]Institute for Telecommunications Research, [†]School of Engineering
University of South Australia, Mawson Lakes SA 5095, Australia

ABSTRACT

Closed-form pseudolinear estimators are computationally attractive alternatives to iterative nonlinear techniques. For time-of-arrival (TOA) based localization, several pseudolinear estimators have been proposed such as the least squares calibration (LSC) estimator, the linear least squares (LLS) estimator, and their best linear unbiased estimator (BLUE) variants (namely, the BLUE-LSC and BLUE-LLS estimators). Despite their stable performance and low computational complexity, these pseudolinear estimators suffer from bias problems due to the nonzero mean of the pseudolinear noise vectors. In this paper, we present a bias analysis for the TOA-based pseudolinear estimators. Based on the bias analysis we develop bias compensation methods that lead to new bias-compensated versions of the LSC, LLS, BLUE-LSC and BLUE-LLS estimators. The superior performance of the proposed bias-compensated estimators is demonstrated via numerical simulations. The new estimators are observed to exhibit negligible estimation bias even at high measurement noise levels.

***Index Terms*—** Time-of-arrival, source localization, sensor array, bias compensation, least squares

1. INTRODUCTION

Source localization has been an area of extensive research for many years due to its wide range of applications in mobile communications, wireless sensor network, search and rescue, radar and sonar, to name but a few. Common localization methods are based on time-of-arrival (TOA) [1–14], angle-of-arrival (AOA) [15–17], time-difference-of-arrival (TDOA) [13, 18–21], Doppler frequency [15, 22–25], and received signal strength (RSS) [26] measurements collected by a number of spatially distributed sensors or a single moving sensor. In this paper, we focus our attention on the problem of source localization in the two-dimensional (2D) plane using TOA measurements obtained from an array of spatially distributed sensors.

In TOA-based localization, the one-way or round-trip propagation time of the signal between the source and each of the sensors is measured, which traces out a circle centred at the sensor position for the possible source positions. With three or more sensors, a unique solution of the source position can be obtained by converting the TOA measurements into a set of circular equations and exploiting the knowledge of the sensor array geometry. To deal with the nonlinearity of the circular TOA equations, iterative approaches are commonly used in the literature such as the Taylor-series method [1] and the steepest descent method [2]. However, the main drawback of these techniques is their computationally demanding iterative nature. In addition, the iterative techniques require a good initial guess that must be sufficiently close to the actual source position to ensure convergence to the global solution. An attractive alternative approach is to algebraically rearrange the nonlinear TOA equations into a set of equations that are linear in the unknowns, thereby allowing the use of least squares (LS) estimation [4–6]. In particular, the reformulated linear equations in the least squares calibration (LSC) method [4] were derived based on the introduction of an extra nuisance parameter which is a function of the source position. On the other hand, the linear least squares (LLS) method [5, 6] relies on subtracting linear LSC equations so as to eliminate the common nuisance parameter and form a set of nuisance-parameter-free linear equations. The performance of the LSC and LLS estimators were improved in [7] by exploiting the best linear unbiased estimator (BLUE) technique, resulting in the BLUE-LSC and BLUE-LLS estimator. It was proved in [7] that the performance of the BLUE-LLS estimator with the linear equations corresponding to an independent set of sensor pairs is identical to that of the BLUE-LLS estimator. Another refinement of the LSC estimator was proposed in [9], namely the constrained weighted LSC (CWLSC) estimator, by imposing a constraint on the relation between the nuisance parameter and the source position. However, the CWLSC estimator requires a significantly higher computational load than the BLUE-LSC and BLUE-LLS estimators [7]. Other localization techniques based on multidimensional scaling, multidimensional similarity and constrained optimization can also be found in the literature (see, e.g., [10–13] and the references therein).

Despite the advantages of low computational complexity and high stability, the closed-form pseudolinear estimators, i.e., the LSC, LLS, BLUE-LSC and BLUE-LLS estimators, proposed in [4–7] suffer from bias. The main reason for the bias problems of the pseudolinear estimators is that the measurement noise vector is no longer zero-mean as a result of the algebraic nonlinear-to-linear transformation of the TOA equations. In this paper, we aim to analyse the bias of the LSC, LLS, BLUE-LSC and BLUE-LLS estimators and propose bias compensation methods by exploiting the mean of the pseudolinear noise vector. The effectiveness of the proposed bias compensation methods is illustrated by way of numerical simulation examples, where the proposed bias-compensated versions of the LSC, LLS, BLUE-LSC and BLUE-LLS estimators are observed to exhibit very small bias even at moderate and high measurement noise levels.

The paper is organized as follows. Section 2 defines the TOA-based localization problem. An overview of closed-form pseudolinear estimators is provided in Section 3 including the LSC, LLS, BLUE-LSC and BLUE-LLS estimators. The bias of these estimators is analysed in Section 4. Section 5 presents the proposed bias compensation methods. Simulation results are presented in Section 6. The paper concludes in Section 7 with a brief summary.

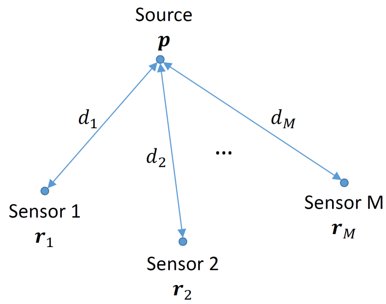

Fig. 1. TOA-based localization geometry with M sensors.

2. PROBLEM FORMULATION

The problem of 2D source localization using TOA measurements is depicted in Fig. 1, where $\mathbf{p} = [p_x, p_y]^T$ is the unknown source position to be determined and $\mathbf{r}_i = [r_{x,i}, r_{y,i}]^T$, $i = 1, 2, \ldots, M$, is the position of the ith sensor. Here, the superscript ^{T} stands for matrix transpose. The one-way TOA measurement obtained at sensor i is given by

$$\tilde{\tau}_i(\mathbf{p}) = \tau_i + e_i \tag{1}$$

where $\tau_i = \frac{\|\mathbf{p}-\mathbf{r}_i\|}{c}$, $\|\cdot\|$ denotes the Euclidean norm, c is the speed of signal propagation, and e_i is the TOA measurement error. For simplicity, the line-of-sight propagation between the source and all the sensors is assumed such that each e_i is a zero-mean independent white process with known variance $\mathbb{E}\{e_i^2\}$. Note that the error variance $\mathbb{E}\{e_i^2\}$ is commonly a function of the source-sensor distance among other things. Given the signal propagation speed c, the range measurement between the source and sensor i can be expressed as

$$\tilde{d}_i(\mathbf{p}) = d_i + n_i \tag{2}$$

where $d_i = \|\mathbf{p} - \mathbf{r}_i\|$ is the true range and $n_i = ce_i$ is the corresponding range measurement error with $\mathbb{E}\{n_i^2\} = \sigma_i^2$ (i.e., $\mathbb{E}\{e_i^2\} = \sigma_i^2/c^2$).

Solving for $\mathbf{p}$ from range measurements $\tilde{d}_1, \ldots, \tilde{d}_M$ requires at least two measurements (i.e., $M \geq 2$) because there are two unknowns p_x and p_y. However, at least three measurements (i.e., $M \geq 3$) are required to ensure the uniqueness of the solution since two TOA circles may intersect at two distinct points.

3. OVERVIEW OF PSEUDOLINEAR ESTIMATORS

3.1. LSC and BLUE-LSC

Squaring both sides of (2) gives [4]

$$r_{x,i}p_x + r_{y,i}p_y - 0.5R = \frac{1}{2}(r_{x,i}^2 + r_{y,i}^2 - \tilde{d}_i^2) + m_i \tag{3}$$

where $R = \|\mathbf{p}\|^2$ is the additional nuisance parameter introduced in the process of arriving at (3) and $m_i = n_i^2/2 + d_i n_i$ is the resulting pseudolinear noise. By stacking the pseudolinear equations (3) for $i = 1, \ldots, M$, we have

$$\mathbf{A}\boldsymbol{\theta} + \boldsymbol{\eta} = \mathbf{b} \tag{4}$$

where

$$\mathbf{A} = \begin{bmatrix} r_{x,1} & r_{y,1} & -0.5 \\ \vdots & \vdots & \vdots \\ r_{x,M} & r_{y,M} & -0.5 \end{bmatrix} \tag{5a}$$

$$\boldsymbol{\theta} = \begin{bmatrix} p_x & p_y & R \end{bmatrix}^T \tag{5b}$$

$$\boldsymbol{\eta} = -\begin{bmatrix} m_1 & \cdots & m_M \end{bmatrix}^T \tag{5c}$$

and

$$\mathbf{b} = \frac{1}{2}\begin{bmatrix} r_{x,1}^2 + r_{y,1}^2 - \tilde{d}_1^2 \\ \vdots \\ r_{x,M}^2 + r_{y,M}^2 - \tilde{d}_M^2 \end{bmatrix}. \tag{5d}$$

Solving (4) for $\boldsymbol{\theta}$ in least squares sense yields [4]

$$\hat{\boldsymbol{\theta}}_{\text{LSC}} = \left(\mathbf{A}^T\mathbf{A}\right)^{-1}\mathbf{A}^T\mathbf{b}, \tag{6}$$

and the LSC estimate of $\mathbf{p}$ can be straightforwardly obtained from $\hat{\boldsymbol{\theta}}_{\text{LSC}}$ as

$$\hat{\mathbf{p}}_{\text{LSC}} = \hat{\boldsymbol{\theta}}_{\text{LSC}}(1:2). \tag{7}$$

Similarly, the BLUE for $\boldsymbol{\theta}$ can be obtained with the use of the covariance matrix $\mathbf{C}_{\boldsymbol{\eta}} = \mathbb{E}\{\boldsymbol{\eta}\boldsymbol{\eta}^T\}$ [7]:

$$\hat{\boldsymbol{\theta}}_{\text{BLUE-LSC}} = \left(\mathbf{A}^T\mathbf{C}_{\boldsymbol{\eta}}^{-1}\mathbf{A}\right)^{-1}\mathbf{A}^T\mathbf{C}_{\boldsymbol{\eta}}^{-1}\mathbf{b} \tag{8}$$

and the BLUE-LSC estimate of $\mathbf{p}$ can be extracted from $\hat{\boldsymbol{\theta}}_{\text{BLUE-LSC}}$ using

$$\hat{\mathbf{p}}_{\text{BLUE-LSC}} = \hat{\boldsymbol{\theta}}_{\text{BLUE-LSC}}(1:2). \tag{9}$$

The covariance matrix $\mathbf{C}_{\boldsymbol{\eta}}$ is approximated by [7]

$$\mathbf{C}_{\boldsymbol{\eta}} \simeq \text{diag}\left(d_1^2\sigma_1^2, \ldots, d_M^2\sigma_M^2\right) \tag{10}$$

for sufficiently small noise levels. Note that the knowledge of d_i, $i = 1, \ldots, M$, is not readily available. Therefore $\tilde{d}_i$ is used instead to compute $\mathbf{C}_{\boldsymbol{\eta}}$.

3.2. LLS and BLUE-LSS

The nuisance parameter R in (3) can be eliminated by writing (3) for the 1st and ith sensors and subtracting the equation for the 1st sensor from the equation for the ith sensor:

$$\begin{aligned}&(r_{x,i} - r_{x,1})p_x + (r_{y,i} - r_{y,1})p_y \\ &= \frac{1}{2}(r_{x,i}^2 + r_{y,i}^2 - r_{x,1}^2 - r_{y,1}^2 - \tilde{d}_i^2 + \tilde{d}_1^2) + m_i - m_1.\end{aligned} \tag{11}$$

Writing (11) in matrix form for $i = 2, \ldots, M$ gives

$$\mathbf{G}\mathbf{p} + \boldsymbol{\epsilon} = \mathbf{h} \tag{12}$$

where

$$\mathbf{G} = \begin{bmatrix} r_{x,2} - r_{x,1} & r_{y,2} - r_{y,1} \\ \vdots & \vdots \\ r_{x,M} - r_{x,1} & r_{y,M} - r_{y,1} \end{bmatrix} \tag{13a}$$

$$\boldsymbol{\epsilon} = \begin{bmatrix} m_1 - m_2 \\ \vdots \\ m_1 - m_M \end{bmatrix} \tag{13b}$$

and

$$\mathbf{h} = \frac{1}{2}\begin{bmatrix} r_{x,2}^2 + r_{y,2}^2 - r_{x,1}^2 - r_{y,1}^2 - \tilde{d}_2^2 + \tilde{d}_1^2 \\ \vdots \\ r_{x,M}^2 + r_{y,M}^2 - r_{x,1}^2 - r_{y,1}^2 - \tilde{d}_M^2 + \tilde{d}_1^2 \end{bmatrix}. \tag{13c}$$

The LLS estimate of $\mathbf{p}$ is now obtained by solving (12) in the LS sense [5,6]:

$$\hat{\mathbf{p}}_{\text{LLS}} = \left(\mathbf{G}^T\mathbf{G}\right)^{-1}\mathbf{G}^T\mathbf{h}, \quad (14)$$

On the other hand, the BLUE-LLS estimate is given by [7]

$$\hat{\mathbf{p}}_{\text{BLUE-LLS}} = \left(\mathbf{G}^T\mathbf{C}_{\boldsymbol{\epsilon}}^{-1}\mathbf{G}\right)^{-1}\mathbf{G}^T\mathbf{C}_{\boldsymbol{\epsilon}}^{-1}\mathbf{h} \quad (15)$$

with the use of the covariance matrix $\mathbf{C}_{\boldsymbol{\epsilon}} = \mathbb{E}\{\boldsymbol{\epsilon}\boldsymbol{\epsilon}^T\}$:

$$\mathbf{C}_{\boldsymbol{\epsilon}} \simeq \begin{bmatrix} d_1^2\sigma_1^2 + d_2^2\sigma_2^2 & d_1^2\sigma_1^2 & \cdots & d_1^2\sigma_1^2 \\ d_1^2\sigma_1^2 & d_1^2\sigma_1^2 + d_3^2\sigma_3^2 & \cdots & d_1^2\sigma_1^2 \\ \vdots & \vdots & \ddots & \vdots \\ d_1^2\sigma_1^2 & d_1^2\sigma_1^2 & \cdots & d_1^2\sigma_1^2 + d_M^2\sigma_M^2 \end{bmatrix} \quad (16)$$

Similar to $\mathbf{C}_{\boldsymbol{\eta}}$, the unknown $d_i, i = 1, \ldots, M$, are replaced by $\tilde{d}_i$ to compute $\mathbf{C}_{\boldsymbol{\epsilon}}$ in practice.

Note that, although the first sensor is chosen here as the reference sensor, the performance of the BLUE-LLS estimator remains the same if an independent set of sensor pairs is used to formulate the LLS equations.

4. BIAS ANALYSIS

By substituting (4) into (6), the LSC estimate $\hat{\boldsymbol{\theta}}_{\text{LSC}}$ of $\boldsymbol{\theta}$ can be expressed as

$$\hat{\boldsymbol{\theta}}_{\text{LSC}} = \boldsymbol{\theta} + \left(\mathbf{A}^T\mathbf{A}\right)^{-1}\mathbf{A}^T\boldsymbol{\eta}. \quad (17)$$

Thus, the bias of $\hat{\boldsymbol{\theta}}_{\text{LSC}}$ is given by

$$\begin{aligned}\boldsymbol{\delta}_{\text{LSC}} &= \mathbb{E}\{\hat{\boldsymbol{\theta}}_{\text{LSC}}\} - \boldsymbol{\theta} \\ &= \left(\mathbf{A}^T\mathbf{A}\right)^{-1}\mathbf{A}^T\mathbb{E}\{\boldsymbol{\eta}\}.\end{aligned} \quad (18)$$

Similarly, the bias of $\hat{\boldsymbol{\theta}}_{\text{BLUE-LSC}}$, $\hat{\mathbf{p}}_{\text{LLS}}$, and $\hat{\mathbf{p}}_{\text{BLUE-LLS}}$ are given by

$$\begin{aligned}\boldsymbol{\delta}_{\text{BLUE-LSC}} &= \mathbb{E}\{\hat{\boldsymbol{\theta}}_{\text{BLUE-LSC}}\} - \boldsymbol{\theta} \\ &= \left(\mathbf{A}^T\mathbf{C}_{\boldsymbol{\eta}}^{-1}\mathbf{A}\right)^{-1}\mathbf{A}^T\mathbf{C}_{\boldsymbol{\eta}}^{-1}\mathbb{E}\{\boldsymbol{\eta}\}, && (19) \\ \boldsymbol{\delta}_{\text{LLS}} &= \mathbb{E}\{\hat{\mathbf{p}}_{\text{LLS}}\} - \mathbf{p} \\ &= \left(\mathbf{G}^T\mathbf{G}\right)^{-1}\mathbf{G}^T\mathbb{E}\{\boldsymbol{\epsilon}\}, && (20) \\ \boldsymbol{\delta}_{\text{BLUE-LLS}} &= \mathbb{E}\{\hat{\mathbf{p}}_{\text{BLUE-LLS}}\} - \mathbf{p} \\ &= \left(\mathbf{G}^T\mathbf{C}_{\boldsymbol{\epsilon}}^{-1}\mathbf{G}\right)^{-1}\mathbf{G}^T\mathbf{C}_{\boldsymbol{\epsilon}}^{-1}\mathbb{E}\{\boldsymbol{\epsilon}\}. && (21)\end{aligned}$$

The algebraic transformation of nonlinear TOA equations causes the pseudolinear noise vectors $\boldsymbol{\eta}$ and $\boldsymbol{\epsilon}$ to have nonzero means:

$$\mathbb{E}\{\boldsymbol{\eta}\} = -\begin{bmatrix}\mathbb{E}\{m_1\} \\ \vdots \\ \mathbb{E}\{m_M\}\end{bmatrix} = -\frac{1}{2}\begin{bmatrix}\sigma_1^2 \\ \vdots \\ \sigma_M^2\end{bmatrix} \neq \mathbf{0} \quad (22a)$$

and

$$\mathbb{E}\{\boldsymbol{\epsilon}\} = \begin{bmatrix}\mathbb{E}\{m_1 - m_2\} \\ \vdots \\ \mathbb{E}\{m_1 - m_M\}\end{bmatrix} = \frac{1}{2}\begin{bmatrix}\sigma_1^2 - \sigma_2^2 \\ \vdots \\ \sigma_1^2 - \sigma_M^2\end{bmatrix} \neq \mathbf{0}. \quad (22b)$$

Note that, since the noise variance σ_i^2 is a function of the source-sensor distance, we have $\sigma_j^2 \neq \sigma_i^2$ in general, therefore leading to $\mathbb{E}\{\boldsymbol{\epsilon}\} \neq \mathbf{0}$.

Consequently, the nonzero mean of $\mathbb{E}\{\boldsymbol{\eta}\}$ and $\mathbb{E}\{\boldsymbol{\epsilon}\}$ in (22) implies that the LSC, LLS, BLUE-LSC and BLUE-LLS estimators are biased (i.e., $\boldsymbol{\delta}_{\text{LSC}} \neq \mathbf{0}$, $\boldsymbol{\delta}_{\text{LLS}} \neq \mathbf{0}$, $\boldsymbol{\delta}_{\text{BLUE-LSC}} \neq \mathbf{0}$ and $\boldsymbol{\delta}_{\text{BLUE-LLS}} \neq \mathbf{0}$).

5. BIAS COMPENSATION

The bias-compensated LSC (BC-LSC) estimate of $\boldsymbol{\theta}$ is obtained by subtracting the bias term $\boldsymbol{\delta}_{\text{LSC}}$ in (18) from the LSC estimate $\hat{\boldsymbol{\theta}}_{\text{LSC}}$ in (14):

$$\hat{\boldsymbol{\theta}}_{\text{BC-LSC}} = \hat{\boldsymbol{\theta}}_{\text{LSC}} - \boldsymbol{\delta}_{\text{LSC}} = \left(\mathbf{A}^T\mathbf{A}\right)^{-1}\mathbf{A}^T\left(\mathbf{b} - \mathbb{E}\{\boldsymbol{\eta}\}\right), \quad (23)$$

and the BC-LSC estimate of $\mathbf{p}$ is consequently extracted from $\hat{\boldsymbol{\theta}}_{\text{BC-LSC}}$ as

$$\hat{\mathbf{p}}_{\text{BC-LSC}} = \hat{\boldsymbol{\theta}}_{\text{BC-LSC}}(1:2). \quad (24)$$

Similarly, the bias-compensated LLS (BC-LLS) estimator is given by

$$\hat{\mathbf{p}}_{\text{BC-LLS}} = \hat{\mathbf{p}}_{\text{LLS}} - \boldsymbol{\delta}_{\text{LLS}} = \left(\mathbf{G}^T\mathbf{G}\right)^{-1}\mathbf{G}^T\left(\mathbf{h} - \mathbb{E}\{\boldsymbol{\epsilon}\}\right). \quad (25)$$

The same bias compensation approach can be applied directly to the BLUE-LSC and BLUE-LSS estimator if the exact expression of the weighting matrices $\mathbf{C}_{\boldsymbol{\eta}}$ in (10) and $\mathbf{C}_{\boldsymbol{\epsilon}}$ in (16) is obtained by using d_i, $i = 1, \ldots, M$, instead of $\tilde{d}_i$. However, the fact that $\tilde{d}_i$ is used to calculate $\mathbf{C}_{\boldsymbol{\eta}}$ and $\mathbf{C}_{\boldsymbol{\epsilon}}$ (since d_i is unknown) may result in undesirable bias performance of the BLUE-LSC and BLUE-LSS estimators in large noise conditions. To avoid this problem, a two-stage bias-compensated BLUE-LSC (BC-BLUE-LSC) estimator is proposed as follows:

1. Compute $\hat{\mathbf{p}}_{\text{BLUE-LSC}}$ using (8) and (9).
2. Compute $\hat{d}_i = \|\hat{\mathbf{p}}_{\text{BLUE-LSC}} - \mathbf{r}_i\|$, $i = 1, \ldots, M$, and construct $\mathbf{C}_{\boldsymbol{\eta}}^{\dagger}$ in (10) using $\hat{d}_i$.
3. Compute

$$\hat{\boldsymbol{\theta}}_{\text{BC-BLUE-LSC}} = \left(\mathbf{A}^T(\mathbf{C}_{\boldsymbol{\eta}}^{\dagger})^{-1}\mathbf{A}\right)^{-1}\mathbf{A}^T(\mathbf{C}_{\boldsymbol{\eta}}^{\dagger})^{-1}\left(\mathbf{b} - \mathbb{E}\{\boldsymbol{\eta}\}\right). \quad (26)$$

4. Extract $\hat{\mathbf{p}}_{\text{BC-BLUE-LSC}} = \hat{\boldsymbol{\theta}}_{\text{BC-BLUE-LSC}}(1:2)$.

Similarly, for the BLUE-LLS method, we have the following two-stage bias-compensated BLUE-LLS (BC-BLUE-LLS) algorithm:

1. Compute $\hat{\mathbf{p}}_{\text{BLUE-LLS}}$ using (15).
2. Compute $\hat{d}_i = \|\hat{\mathbf{p}}_{\text{BLUE-LLS}} - \mathbf{r}_i\|$, $i = 1, \ldots, M$, and construct $\mathbf{C}_{\boldsymbol{\epsilon}}^{\dagger}$ in (16) using $\hat{d}_i$.
3. Compute

$$\hat{\mathbf{p}}_{\text{BC-BLUE-LLS}} = \left(\mathbf{G}^T(\mathbf{C}_{\boldsymbol{\epsilon}}^{\dagger})^{-1}\mathbf{G}\right)^{-1}\mathbf{G}^T(\mathbf{C}_{\boldsymbol{\epsilon}}^{\dagger})^{-1}\left(\mathbf{h} - \mathbb{E}\{\boldsymbol{\epsilon}\}\right). \quad (27)$$

6. SIMULATION STUDIES

In this section, we demonstrate the performance of the proposed bias-compensated pseudolinear estimators, viz., the BC-LSC, BC-LLS, BC-BLUE-LSC and BC-BLUE-LLS estimators, in comparison to the conventional LSC, LLS, BLUE-LSC and BLUE-LLS estimators, by way of Monte Carlo simulations. We consider a simulated TOA-based localization scenario with a source located at $\mathbf{p} = [0, -3000]^T$ m and four sensors located at $\mathbf{r}_1 = [3000, 3000]^T$ m, $\mathbf{r}_2 = [-3000, 3000]^T$ m, $\mathbf{r}_3 = [-3000, -3000]^T$ m, and $\mathbf{r}_4 = [3000, -3000]^T$ m. The measurement error variance at each sensor is range-dependent and modelled as $\sigma_i^2 = \sigma_0^2 d_i^2/d_0^2$, where $\sigma_0 \in \{20, 40, 60, 80, 100\}$ m is the reference variance and $d_0 = 1000$ m is the reference range.

Table 1. Bias Performance

σ_0 (m)	Bias norm (m)							
	LSC	BC-LSC	LLS	BC-LLS	BLUE-LSC	BC-BLUE-LSC	BLUE-LLS	BC-BLUE-LLS
20	1.2174	0.1906	1.1612	0.2705	1.6590	0.0070	1.6590	0.0070
40	4.7480	0.2121	4.6853	0.2971	6.6756	0.0625	6.6756	0.0625
60	11.0671	0.4450	11.2179	0.6487	14.5049	0.2649	14.5049	0.2649
80	19.7096	0.8696	19.5617	0.9331	25.7279	0.5826	25.7279	0.5826
100	29.9931	0.0984	30.0149	0.0777	40.4164	0.1685	40.4164	0.1685

Table 2. RMSE Performance

σ_0 (m)	RMSE (m)								BLUE Bound[(a)]	CRLB[(b)]
	LSC	BC-LSC	LLS	BC-LLS	BLUE-LSC	BC-BLUE-LSC	BLUE-LLS	BC-BLUE-LLS		
20	153.0575	153.0527	182.2563	182.2529	115.9787	115.9440	115.9787	115.9440	115.8912	113.9332
40	306.0218	305.9850	364.5240	364.4940	232.0843	231.7393	232.0843	231.7393	231.7824	227.8664
60	459.2532	459.1201	546.8693	546.7546	348.9682	347.9188	348.9682	347.9188	347.6736	341.7995
80	613.8229	613.5070	731.0536	730.7925	467.3568	464.8881	467.3568	464.8881	463.5648	455.7327
100	767.3943	766.8080	913.8549	913.3619	585.5170	580.8790	585.5170	580.8790	579.4560	569.6659

(a) the square root of the trace of the theoretical covariance matrix of the BLUE-LSC and BLUE-LLS estimators

(b) the square root of the trace of the CRLB matrix estimators

For performance comparison, the bias norm and root mean squared error (RMSE) of the estimators are estimated via 1,000,000 Monte Carlo simulation runs. The bias norm is defined by $\|\mathbb{E}\{\hat{\mathbf{p}}_{\mathrm{X}}\}-\mathbf{p}\|$ while the RMSE is defined by $\left(\operatorname{tr}\mathbb{E}\{(\hat{\mathbf{p}}_{\mathrm{X}}-\mathbf{p})(\hat{\mathbf{p}}_{\mathrm{X}}-\mathbf{p})^T\}\right)^{1/2}$, where $\hat{\mathbf{p}}_{\mathrm{X}}$ is a position estimate under consideration. In addition, the square root of the trace of the theoretical covariance matrix of the TOA-based BLUE estimators and the square root of the trace of the CRLB matrix are also computed as performance benchmarks. The theoretical covariance matrices of the source position estimates obtained by the BLUE-LSC estimator and the BLUE-LLS estimator with an independent set of sensor pairs are identical and given by [7]

$$\mathbf{C}_{\mathbf{p}} \simeq \left(\mathbf{G}^T\mathbf{C}_{\boldsymbol{\epsilon}}^{-1}\mathbf{G}\right)^{-1}. \tag{28}$$

The CRLB matrix for TOA-based localization has the expression of

$$\mathrm{CRLB} = \left(\mathbf{J}^T\mathbf{K}^{-1}\mathbf{J}\right)^{-1} \tag{29}$$

where $\mathbf{K} = \operatorname{diag}(\sigma_1^2, \ldots, \sigma_M^2)$ is the covariance matrix of the measurement vector $\mathbf{n} = [n_1, \ldots, n_M]^T$, and $\mathbf{J} = [\mathbf{J}_1^T, \ldots, \mathbf{J}_M^T]^T$ with $\mathbf{J}_i = (\mathbf{p}^T - \mathbf{r}_i^T)/\|\mathbf{p}-\mathbf{r}_i\|$ is the Jacobian matrix evaluated at the true source position $\mathbf{p}$.

Table 1 shows the bias performance of the proposed BC-LSC, BC-LLS, BC-BLUE-LSC and BC-BLUE-LLS estimators in comparison to that of the conventional LSC, LLS, BLUE-LSC and BLUE-LLS estimators for $\sigma_0 \in \{20, 40, 60, 80, 100\}$ m. It is observed from Table 1 that the conventional LSC, LLS, BLUE-LSC and BLUE-LLS estimators suffer from bias problems and their bias norms become significantly large as the measurement noise is increased. In contrast, by taking into account the nonzero mean of the pseudolinear noise vector, the proposed BC-LSC, BC-LLS, BC-BLUE-LSC and BC-BLUE-LLS estimators exhibit negligible bias even for large measurement noise levels. This confirms the effectiveness of the proposed bias-compensation methods in ameliorating the bias problem associated with the conventional LSC, LLS, BLUE-LSC and BLUE-LLS estimators.

Table 2 shows the RMSE performance of the estimators for $\sigma_0 \in \{20, 40, 60, 80, 100\}$ m. In addition to the bias performance advantage as discussed above, the proposed BC-LSC, BC-LLS, BC-BLUE-LSC and BC-BLUE-LLS estimators appear to slightly outperform the corresponding LSC, LLS, BLUE-LSC and BLUE-LLS estimators, respectively. Moreover, the BLUE-LSC and BLUE-LLS estimators as well as the BC-BLUE-LSC and BC-BLUE-LLS estimators exhibit RMSE performance in agreement with the theoretical BLUE covariance matrix. In addition, it is also observed that their RMSE performance is slightly worse than the CRLB. This observation is consistent with the suboptimality of these types of estimators that has been discussed in [7].

7. CONCLUSION

Despite their low computational complexity and stable performance, the closed-form pseudolinear estimators for TOA-based localization are plagued by bias problems due to the nonzero mean of the pseudolinear noise vector resulting from the transformation of the nonlinear TOA measurement equations. In this paper, we have analysed the bias properties of the LSC, LLS, BLUE-LSC and BLUE-LLS estimators. In addition, we proposed bias compensation methods exploiting the mean of the pseudolinear noise vector, resulting in four new bias-compensated pseudolinear estimators for TOA localization; viz., the BC-LSC, BC-LLS, BC-BLUE-LSC and BC-BLUE-LLS estimators. The performance of proposed bias compensation methods was demonstrated by way of numerical Monte Carlo simulations. Specifically, it was observed that, in contrast to the conventional LSC, LLS, BLUE-LSC and BLUE-LLS estimators that suffer from severe estimation bias at moderate and large noise levels, the proposed BC-LSC, BC-LLS, BC-BLUE-LSC and BC-BLUE-LLS estimators exhibit negligible bias even in large noise conditions.

8. REFERENCES

[1] M. A. Spirito, "On the accuracy of cellular mobile station location estimation," *IEEE Trans. Veh. Technol.*, vol. 50, no. 3, pp. 674–685, May 2001.

[2] J. Caffery and G. L. Stuber, "Subscriber location in CDMA cellular networks," *IEEE Trans. Veh. Technol.*, vol. 47, no. 2, pp. 406–416, May 1998.

[3] N. H. Nguyen and K. Dogancay, "Optimal geometry analysis for multistatic TOA localization," *IEEE Trans. Signal Process.*, vol. 64, no. 16, pp. 4180–4193, Aug. 2016.

[4] J. C. Chen, R. E. Hudson, and K. Yao, "Maximum-likelihood source localization and unknown sensor location estimation for wideband signals in the near-field," *IEEE Trans. Signal Process.*, vol. 50, no. 8, pp. 1843–1854, Aug. 2002.

[5] A. J. Fenwick, "Algorithms for position fixing using pulse arrival times," *IEE Proc. - Radar, Sonar Navig.*, vol. 146, no. 4, pp. 208–212, Aug. 1999.

[6] J. J. Caffery, "A new approach to the geometry of TOA location," in *Proc. IEEE Veh. Technol. Conf.*, Boston, MA, Sept. 2000, vol. 4, pp. 1943–1949.

[7] F. K. W. Chan, H. C. So, J. Zheng, and K. W. K. Lui, "Best linear unbiased estimator approach for time-of-arrival based localisation," *IET Signal Process.*, vol. 2, no. 2, pp. 156–162, June 2008.

[8] N. H. Nguyen and K. Dogancay, "Optimal geometry analysis for elliptic target localization by multistatic radar with independent bistatic channels," in *Proc. IEEE Int. Conf. Acoust., Speech, Signal Process.*, Brisbane, Australia, Apr. 2015, pp. 2764–2768.

[9] K. W. Cheung, H. C. So, W. K. Ma, and Y. T. Chan, "Least squares algorithms for time-of-arrival-based mobile location," *IEEE Trans. Signal Process.*, vol. 52, no. 4, pp. 1121–1130, Apr. 2004.

[10] K. W. Cheung and H. C. So, "A multidimensional scaling framework for mobile location using time-of-arrival measurements," *IEEE Trans. Signal Process.*, vol. 53, no. 2, pp. 460–470, Feb. 2005.

[11] Q. Wan, Y.-J. Luo, W.-L. Yang, J. Xu, J. Tang, and Y.-N. Peng, "Mobile localization method based on multidimensional similarity analysis," in *Proc. IEEE Int. Conf. Acoust., Speech, Signal Process.*, Philadelphia, PA, Mar. 2005, vol. 4, pp. 1081–1084.

[12] H. C. So and F. K. W. Chan, "A generalized subspace approach for mobile positioning with time-of-arrival measurements," *IEEE Trans. Signal Process.*, vol. 55, no. 10, pp. 5103–5107, Oct. 2007.

[13] A. Beck, P. Stoica, and J. Li, "Exact and approximate solutions of source localization problems," *IEEE Trans. Signal Process.*, vol. 56, no. 5, pp. 1770–1778, May 2008.

[14] L. Rui and K. C. Ho, "Elliptic localization: Performance study and optimum receiver placement," *IEEE Trans. Signal Process.*, vol. 62, no. 18, pp. 4673–4688, Sept. 2014.

[15] N. H. Nguyen and K. Dogancay, "Single-platform passive emitter localization with bearing and Doppler-shift measurements using pseudolinear estimation techniques," *Signal Process.*, vol. 125, pp. 336–348, 2016.

[16] D. J. Torrieri, "Statistical theory of passive location systems," *IEEE Trans. Aerosp. Electron. Syst.*, vol. 20, no. 2, pp. 183–198, Mar. 1984.

[17] K. Dogancay and H. Hmam, "Optimal angular sensor separation for AOA localization," *Signal Process.*, vol. 88, no. 5, pp. 1248–1260, 2008.

[18] K. Dogancay and N. H. Nguyen, "Low-complexity weighted pseudolinear estimator for TDOA localization with systematic error correction," in *Proc. European Signal Process. Conf. (EUSIPCO)*, Budapest, Hungary, Aug. 2016, pp. 2086–2090.

[19] Y. T. Chan and K. C. Ho, "A simple and efficient estimator for hyperbolic location," *IEEE Trans. Signal Process.*, vol. 42, no. 8, pp. 1905–1915, Aug. 1994.

[20] K. Dogancay, "Emitter localization using clustering-based bearing association," *IEEE Trans. Aerosp. Electron. Syst.*, vol. 41, no. 2, pp. 525–536, Apr. 2005.

[21] K. C. Ho, "Bias reduction for an explicit solution of source localization using TDOA," *IEEE Transactions on Signal Processing*, vol. 60, no. 5, pp. 2101–2114, May 2012.

[22] N. H. Nguyen and K. Dogancay, "Optimal sensor-target geometries for Doppler-shift target localization," in *Proc. European Signal Process. Conf. (EUSIPCO)*, Nice, France, Aug. 2015, pp. 180–184.

[23] K. C. Ho and W. Xu, "An accurate algebraic solution for moving source location using TDOA and FDOA measurements," *IEEE Trans. Signal Process.*, vol. 52, no. 9, pp. 2453–2463, Sept. 2004.

[24] N. H. Nguyen and K. Dogancay, "Algebraic solution for stationary emitter geolocation by a LEO satellite using Doppler frequency measurements," in *Proc. IEEE Int. Conf. Acoust., Speech, Signal Process.*, Shanghai, China, Mar. 2016, pp. 3341–3345.

[25] N. H. Nguyen and K. Dogancay, "Optimal sensor placement for Doppler shift target localization," in *Proc. 2015 IEEE Radar Conf. (RadarCon)*, Arlington VA, USA, May 2015, pp. 1677–1682.

[26] H. C. So and L. Lin, "Linear least squares approach for accurate received signal strength based source localization," *IEEE Trans. Signal Process.*, vol. 59, no. 8, pp. 4035–4040, Aug. 2011.